Radiolocation and Tracking of Automatic Identification System Signals for Maritime Situational Awareness

F. Papi[1], D. Tarchi[1], M.Vespe[1], F. Oliveri[1], F. Borghese[2], G. Aulicino[3], A. Vollero[3]

[1] European Commission, Joint Research Centre (JRC), Institute for the Protection and Security of the Citizen (IPSC), Maritime Affairs Unit, Via Enrico Fermi 2749, 21027, Ispra (VA), Italy.

[2] Elman s.r.l., Via di valle Caia km 4.7, Pomezia (Rome), Italy.

[3] Italian Coast Guard, Viale dell'Arte 16, Rome, Italy.

Keywords: AIS, Radiolocation, TDOA, EKF

Abstract

The Automatic Identification System (AIS), a ship reporting system originally designed for collision avoidance, is becoming a cornerstone of maritime situational awareness. The recent increase of terrestrial networks and satellite constellations of receivers is providing global tracking data that enable a wide spectrum of applications beyond collision avoidance. Nevertheless, AIS suffers the lack of security measures that makes it prone to receiving positions that are unintentionally incorrect, jammed or deliberately falsified. In this work we analyse a solution to the problem of AIS data verification that can be implemented within a generic networks of ground AIS base stations with no need for additional sensors or technologies.

The proposed approach combines a classic radio-localisation method based on Time Difference of Arrival (TDoA) with an Extended Kalman Filter (EKF) designed to track vessels in geodetic coordinates.

The approach is validated using anonymised real AIS data collected by multiple base stations that partly share coverage areas. The results show a deviation between the estimated origin of detected signals and the broadcast position data in the order of hundreds of meters, therefore demonstrating the operational potential of the methodology.

Introduction

The verification of the trustworthiness of Automatic Identification System (AIS) data is becoming a key problem to exploit the full potential of this technology not only for safety but also for security applications. AIS, originally conceived for collision avoidance, is a system whereby ships broadcast their presence,

identification and location. Differently to other operational coastal active systems for maritime surveillance, AIS is characterised by considerable coverage (VHF propagation) together with a relatively accurate positioning (GNSS) performance [1]. Nevertheless, the cooperative nature of AIS and the lack of intrinsic security make it vulnerable to false or missing declarations.

Ships of 300 gross tons and upwards in international voyages, 500 tons and upwards for cargoes not in international waters and passenger vessels are obliged to be fitted with AIS equipment as regulated by the IMO Safety of life and sea (SOLAS) [2]. Furthermore, all EU fishing vessels of overall length exceeding 15 metres are also required to be fitted with AIS from May 2014 [3].

AIS reports encode state vector information such as latitude, longitude, Speed Over Ground (SOG), Course Over Ground (COG) as derived by the on board GNSS receiver. Such information is broadcast at a variable transmission rate depending on the vessel motion: as an example, the rate is increased up to a message every two seconds when the vessel is sailing at high speed or manoeuvring. In addition, every six minutes, vessels transmit their identification (IMO and MMSI number, ship name and call sign), static (size, type of vessel, type of cargo, etc.) and voyage related information (*e.g.* Estimated Time of Arrival and destination). Such information is manually set and therefore not fully reliable since more subject to errors if compared to positioning data [4].

With the advent of networked regional base stations (*e.g.* the European SafeSeaNet or the Mediterranean AIS Regional Exchange System - MAREΣ), and satellite receiver constellations [5], the system progressively proved effective for maritime surveillance and traffic monitoring, enabling far-reaching applications such as traffic knowledge discovery, route prediction and anomaly detection. The latter can target particular low-likelihood motion trajectories ([6],[7]), alerts such as sailing in restricted areas, abrupt changes of direction (an extensive overview of this rules is presented in [8]) or anomalies related to wrong AIS message information either unintentional or deliberate such as *spoofing*. As an example, false GNSS tracking information can be produced to simulate specific trajectories [9] or false AIS messages can be generated and transmitted at VHF as recently demonstrated in [10]. Such events, besides being potentially serious hazards to the safety of navigation especially in reduced visibility conditions, can also represent security threats by covering unauthorised activities at sea such as illegal movements of goods and people.

The detection of position reporting anomalies either linked to AIS transponder failures or due to deliberately falsified broadcast dynamic information, can be approached in different ways. The correlation with additional sensors can be used to detect AIS data spoofing; such sensors could be coastal radars (see *e.g.* [11]), HF Surface Wave Radars [12] or space based Synthetic Aperture Radar (SAR) [13]. Nevertheless, the operational usability of such approaches depends on the availability and persistency of the data provided by such additional sensors. Similar considerations apply to data correlation using secondary reporting systems such as Long Range Identification and Tracking (LRIT). Other approaches aim at increasing the trustworthiness of the transponder through the use of additional on-board instrumentation as investigated by [14].

In this work we consider a methodology that can be easily applied to the existing AIS network using the messages normally provided by the AIS base stations. The idea is to combine Time of Arrival (ToA) measurements from multiple AIS channels to determine Time Difference of Arrival (TDoA) measurements. Then TDoAs are processed using a classic multilateration procedure [15] to estimate the vessel position with uncertainty at each time instant [16]. Similar approaches based on multilateration (MLAT) and wide area MLAT (WAMT) techniques have been widely used for air traffic surveillance using secondary surveillance radar (SSR) Mode S replies (*e.g.* [17]) leading to location errors in the order of a few metres (see *e.g.* [18]). Differently from such applications, the localisation accuracy that can be achieved using AIS messages is significantly poor as the Cramer-Rao Lower Bound of the ToA estimate using such transmissions is limited by a signal bandwidth that is less than 25 kHz. This is further analysed in the following Sections. Moreover, being the proposed approach leveraging existing systems, the receiving base stations are separated by baselines of tens or even hundreds of kilometres, their number is critically limited to a few units and in principle *ad hoc* deployments are not envisaged. Finally, the VHF radio propagation is often characterised by ducting effects that help in extending the AIS reception far beyond the line-of-sight, but also lead to additional uncertainty on the relationship between the message time of flight and the actual emission location. All the above make multilateration in this context not sufficient to guarantee anti-spoofing operational requirements in terms of location accuracy and coverage areas. As a consequence, a further AIS emission tracking stage is needed after classic multilateration approaches, whereby radiolocation accuracy is improved through time integration by means of an Extended Kalman Filter (EKF) in geodetic coordinates.

This is made possible in the maritime domain as a consequence the relatively slow and predictable manoeuvres of ships with respect to the AIS messages refresh rates.

The paper aims at demonstrating the feasibility of radiolocation of AIS emissions as the basis for future anti-spoofing and AIS verification applications based on anomaly detection techniques.

The paper is organized as follows: in Section 2 we briefly describe the Italian AIS Network; in Section 3 we introduce the models for ToA and TDoA measurements, and discuss the effects of noise with a specific attention towards bias compensation. In Section 4 we define the TDoA based multilateration procedure and discuss some localisation results for different AIS network configurations. The EKF for time integration in geodetic coordinates is discussed in Section 5 along with the tracking results from processing real AIS data collected by the Italian AIS network. Finally, conclusions and future directions are discussed in Section 6.

2. **The Italian AIS Terrestrial Network**

Implemented in 2005 to fulfil the requirements of the Directive 2002/59/EC of the European Parliament and of the Council of 27 June 2002, the Italian AIS network has been completely upgraded in 2012-2103, with the aim to comply with the most recent relevant guidelines and recommendations, such as the IALA Recommendation A 124 on “The AIS Service” (December 2012) and the ITU Recommendation ITU-R M.1371-4 issued on April 2010. The network currently consists of 60 base stations mainly located to get the best VHF coverage (up to 100 nautical miles, even without the duct effect).

The base stations were placed in such a way to get an overlap of the radio coverage (Figure 1) in order to: *i*) increase the overall availability of the services provided by the national AIS network *ii*) enable future adoption of anti-spoofing techniques to improve quality of AIS information received. The overall architecture of the Italian AIS network is shown in Figure 2. One of the key elements of the network is the so called AIS Embedded Server, a fully solid-state device featuring two separate servers thus supporting redundancy or the simultaneous interface to two TCP networks. The AIS Embedded Server, acting as a PSS Controlling Unit (PCU) according to the IALA Recommendation A-124, allows the integration of one or more base stations and their management from shore systems. The Embedded Server can acquire AIS data from the serial ports and from TCP connections according to the specified configuration.

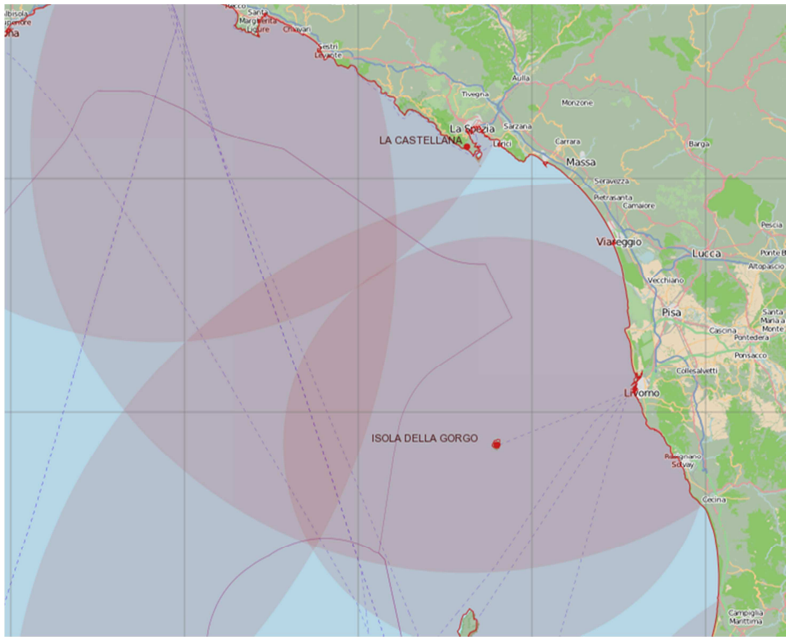

Figure 1: *AIS Coverage Overlapping*

In the same way, the collected AIS data are made available to serial ports and TCP connections. It also features an embedded interface for each web server which allows configuring and monitoring for both the servers and the connected AIS Base Station, without using any additional software. Authorized operators can log-in on the web interface to configure and monitor every aspect of the server, its ports and connections and the linked devices and users.

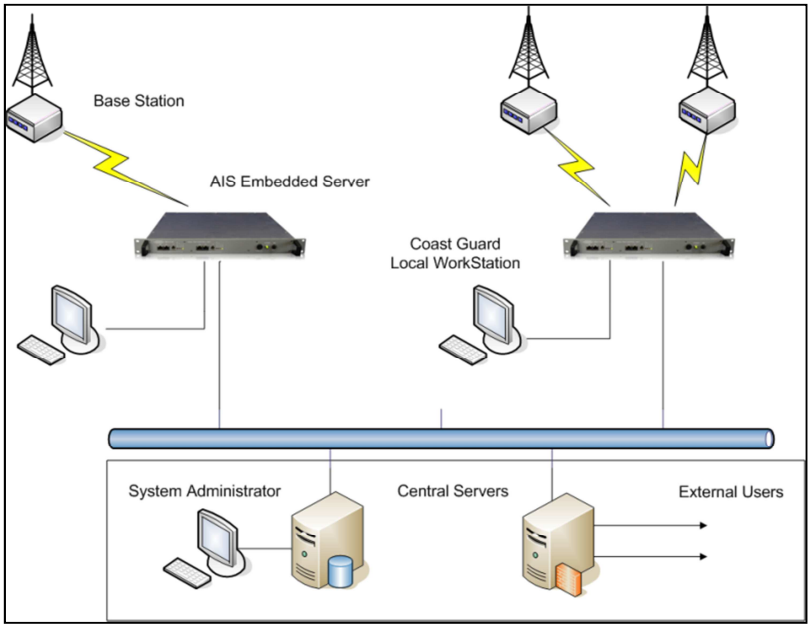

Figure 2*: The Italian AIS Network architecture*

The AIS system dynamically configures into cells using a Self-Organised Time Division Multiple Access (SO-TDMA) scheme. The cell size is adjusted to adapt as a function of the traffic density: in highly congested areas for instance, it is necessary to reduce the size of the cell to diminish the number of transmitter in the cell; this is achieved by reducing the power of the AIS transponders from 12.5 W ('high setting') to 1W ('low setting') thus avoiding message collisions [19]. AIS data are transmitted at a rate of 9.6 kb/s using Gaussian minimum shift keying (GMSK) modulation over two channels 161.975 MHz and 162.025 MHz. For each channel, 2250 slots are allocated within a timeframe of 60 seconds, starting every minute. The bandwidth of the channels is nominally 25 kHz, although the AIS signal spectrum has to be within an emission mask defined by -25 dBc at +10kHz and -70 dBc+25 kHz [19]. Moreover, transmissions of AIS devices are synchronized by using a common time reference, UTC (Coordinated Universal Time), provided by the internal GNSS receiver. Transmission timing error including jitter and systematic offsets should be within ± 104 μs of the synchronisation source for mobile stations and ± 52 μs for base stations, setting the limits of the accuracy of time of flight estimation. If the internal GNSS receiver is faulty, the AIS devices are capable of synchronizing to secondary timing sources as the received AIS messages; in this case, the timing error may increase up to 312 μs. Anyway, AIS stations are not allowed to discard received messages basing upon timing error, even when it is much bigger than the above specified values.

3. ToA and TDoA Measurements

In this section we discuss the models used to describe ToA and TDoA measurements available from the Italian AIS Network. Specific attention is devoted to the analysis of the noise distributions in order to verify stationary and Gaussian assumptions and obtain reasonable estimates for bias compensation.

The standard for AIS base stations provides for a sentence containing information associated to the time of arrival of received messages, expanding the set of messages defined in the NMEA standard [20]. The specific field in the sentence allows representing a precision up to 1 ns, however a precision of 1 μs is currently obtained for the Italian Coast Guard National AIS network. Such precision is sufficient to estimate the location of the emission using multilateration and triangulation techniques as further discussed in this work. The time of arrival is estimated by detecting the position of a specific marker in the AIS message, the start flag, relative to the slot start. The measurement is impacted by the timing error of the receiving station and

by the quality of received signal. Low SNR may affect the accuracy of symbol clock recovery performed by the GMSK demodulator, which is currently limited by a resolution of 10.4 μs set by the internal sampling rate. Eventually, the accuracy of time of arrival may be greatly enhanced by base stations specifically designed to address this issue.

The Time of Flight (*ToF*) of the electromagnetic wave carrying the AIS message can be calculated as the difference between the Time of Arrival (*ToA*) and the beginning of the time slot (T_{slot}) during which the message has been transmitted, *i.e.*:

(1) $$ToF = ToA - T_{slot} - \eta_{tx} - \eta_{rx}$$

where η_{tx} and η_{rx} are the transmitter and receiver timing errors, respectively. When it is possible to fully characterise the errors η_{tx} and η_{rx}, an unbiased estimate of the *ToF* could be obtained and used to derive distance *R* from the considered vessel and the receiving AIS Base Station (AIS-BS), *i.e.* $R=c\ ToF$ where *c* is the speed of light. Multiple distances from different AIS-BSs could then be used to find an unbiased estimate of the instantaneous vessel position using *ToA* based triangulation.

Unfortunately the transmitter timing error η_{tx} is generally unknown and, as mentioned before, can be in the order of tens of μs leading to large ranging uncertainties. Moreover, η_{tx} is vessel-dependent due to differences in the electronics of different transmission equipment. This means that a full characterisation of η_{tx} is not possible and the *ToA* measurements cannot be robustly used to directly solve the vessel localisation problem. The simplest idea in this case is to compare the received *ToAs* pairwise and use the Time Difference of Arrivals (*TDOAs*). Hence, assume the vessel under surveillance is within the coverage area of *n* AIS-BSs, then it is possible to collect $K = \binom{n}{2}$ *TDOAs*, *i.e.*:

$$\hat{ToA}_i = ToA_i + \eta_{tx} + \eta_{rx_i}$$
$$\hat{ToA}_j = ToA_j + \eta_{tx} + \eta_{rx_j}$$

(2) $$TDoA_{i,j} = ToA_i - ToA_j + \eta_{rx_i} - \eta_{rx_j}, \quad 1 \le j < i \le n$$

where $\eta_{rx_i} \sim N(\mu_i, \sigma_i^2)$ and $\eta_{rx_j} \sim N(\mu_j, \sigma_j^2)$ are the receiver timing errors for the *i*-th and *j*-th AIS-BS respectively. We can then rewrite the *TDOAs* vector as follows:

(3) $$TDoA = \begin{bmatrix} TDoA_{2,1} \\ \vdots \\ TDoA_{n,1} \\ TDoA_{3,2} \\ \vdots \\ TDoA_{n,n-1} \end{bmatrix} + v, \qquad v \sim N(\mu_{TDoA}, R_{TDoA})$$

(4) $$\mu_{TDoA} = [\mu_2 - \mu_1 \quad \dots \quad \mu_3 - \mu_2 \quad \dots \quad \mu_n - \mu_{n-1}]$$

(5) $$R_{TDoA} = blockdiag(R_1, R_2, \cdots, R_K)$$

(6) $$R_1 = \begin{bmatrix} \sigma_1^2 + \sigma_2^2 & \cdots & \sigma_1^2 \\ \vdots & \ddots & \vdots \\ \sigma_1^2 & \cdots & \sigma_1^2 + \sigma_n^2 \end{bmatrix}$$

(7) $$R_2 = \begin{bmatrix} \sigma_2^2 + \sigma_3^2 & \cdots & \sigma_2^2 \\ \vdots & \ddots & \vdots \\ \sigma_2^2 & \cdots & \sigma_2^2 + \sigma_n^2 \end{bmatrix}$$

(8) $$R_K = \sigma_n^2 + \sigma_{n-1}^2$$

As for the parameters (μ_i, σ_i) some *a priori* knowledge might be available from the receivers' characteristics. Since this is not our case, an estimate of (μ_{TDoA}, R_{TDoA}) can be obtained using batch data or over a moving time-window. In addition, if ToA measurements are optimally obtained using correlation processing, the standard deviations σ_i can be modelled using the Cramer-Rao Lower Bound [21]:

(9) $$\sigma_i \geq \frac{c}{B \cdot \sqrt{SNR_i}}$$

where *B* is the signal bandwidth and SNR_i is the Signal-to-Noise ratio of the *i*-th channel. SNR_i could be modelled by means of Friis transmission equation as $\hat{SNR}_i = SNR_i(\hat{x}_k)$, where $\hat{x}_k$ is the estimated vessel position at time k.

A noise analysis was performed using real AIS data collected for approximately *9* hours over *3* days. Results are depicted in Figure 3 for a subset of the Italian AIS Network. Both AIS service messages (*i.e.* base station reports periodically transmitted [10]) and AIS messages from verified vessel trajectories were used to estimate the noise distribution.

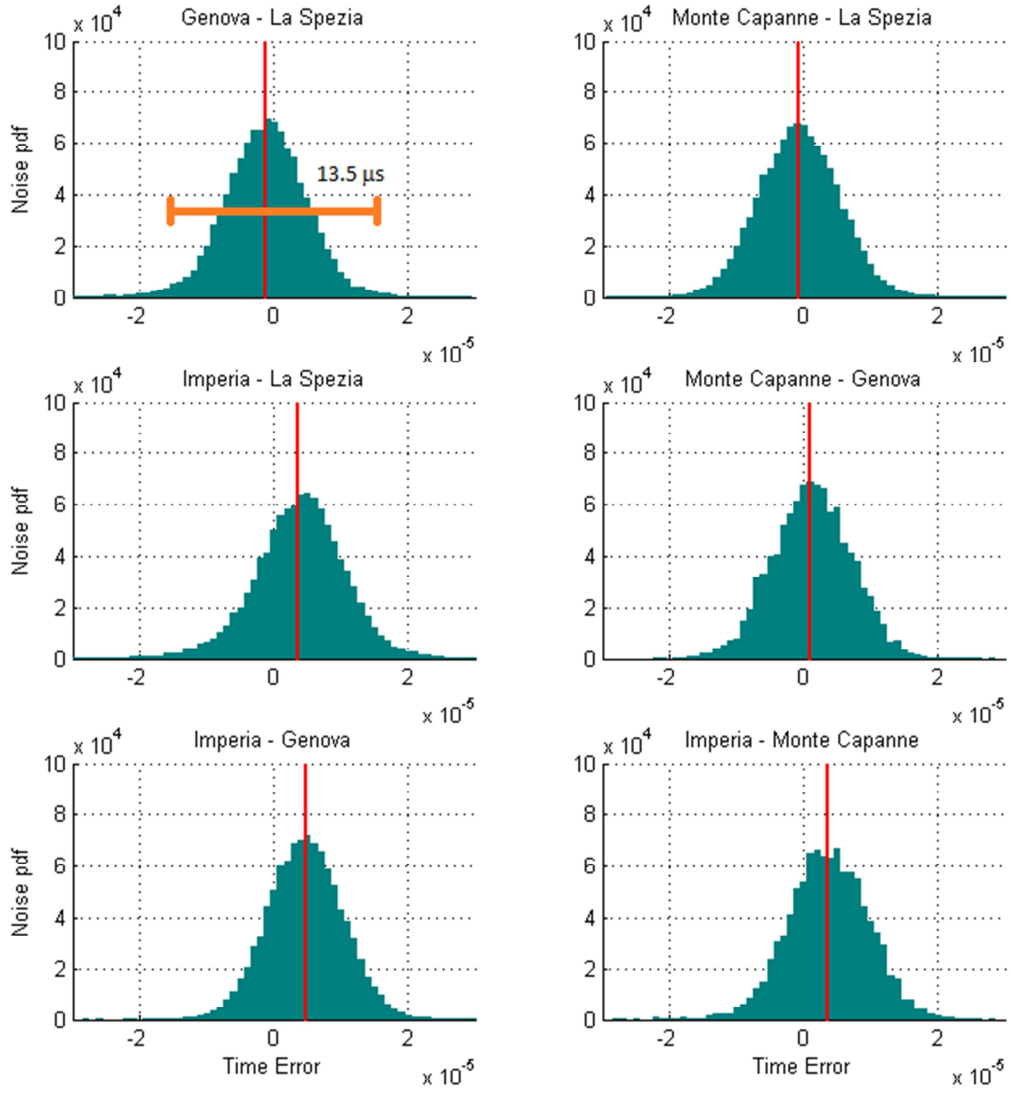

Figure 3: *Probability density function of the TDoA errors for a set of receiving station pairs. The relevant bias $\mu_i - \mu_j$ (highlighted in red) can be readily estimated. Notice also that an upper bound of ±13.5 µs (highlighted in orange) can be selected so that about 95% of noise pdf is included.*

From the results in Figure 3, it is immediate to verify the assumed Gaussian properties and extract reasonable estimates for each bias $\mu_i - \mu_j$ and variance $\sigma_i^2 + \sigma_j^2$. Finally, since the bias μ_{TDoA} appears to be sufficiently stationary we can use the estimate $\hat{\mu}_{TDoA}$ for bias compensation.

4. TDOA-based Vessel Localisation

The problem of estimating an emitter position from *TDoA* measurements occurs in a wide range of applications. Conceptually, a correlation analysis of the received signal from two receivers should give rise to one hyperbolic function. However, due to *TDoA* measurement uncertainty, it is not possible to use multiple hyperbolas to robustly determine a unique intersection [16]. We in fact face a nonlinear estimation problem defined as follows. Assume that a vessel transmitting AIS messages is located at position $P_v = (x_v, y_v)$. Let $P = (x, y)$ be a generic point in geodetic coordinates and let $P_i^{RX} = \left(x_i^{RX}, y_i^{RX}\right)$ be the position vector for the *i*-th AIS base station. Then a nonlinear estimate of P_v is found as:

$$\hat{P}_v = \arg\min_{P} \sum_{i>j} d\left(TDoA_{i,j}, h\left(P, P_i^{RX}, P_j^{RX}\right)\right) \tag{10}$$

where

$$h\left(P, P_i^{RX}, P_j^{RX}\right) = \left(\sqrt{\left(x - x_i^{RX}\right)^2 + \left(y - y_i^{RX}\right)^2} - \sqrt{\left(x - x_j^{RX}\right)^2 + \left(y - y_j^{RX}\right)^2}\right) \Big/ c \tag{11}$$

and $d(\cdot)$ is a suitable distance. This could be for instance the square of the Euclidean distance (*i.e.* least squares estimate) or the Mahalanobis distance (*i.e.* maximum likelihood estimate).

Since we are instead interested in finding the associated estimation error we can use the following approach. Consider for instance a fixed grid of points *P* in geodetic coordinates, and set an upper bound on the differential time uncertainty as $K = 13.5\mu s$, which corresponds to about 4 km location uncertainty. This bound was chosen so that *95%* of the noise *probability density function* (pdf) is covered (see Figure 3). Then we can easily identify the set of points *P* that satisfy the following set of inequalities, *i.e.*

$$\left| h\left(P, P_i^{RX}, P_j^{RX}\right) - TDoA_{i,j} \right| \le c \cdot K, \qquad 1 \le j < i \le n \tag{12}$$

The locus of points where (12) is verified is a hyperbola with uncertainty in the flat-earth approximation case [16]. The area contained by all intersections can be thought of as a measure of the estimation error. Examples of this are shown in Figure 4 and Figure 5 where the AIS message emission is located within the intersection of the hyperbolic functions as derived from the *TDoA* measurements between three and four stations respectively.

Then assuming a Gaussian distribution for the noise terms (as verified in the previous section), the associated estimation covariance is given by the minimum volume ellipse enclosing all points that verified (12).

A more rigorous approach uses the Mahalanobis distance:

$$
\begin{aligned}
& d_{i,j}^{M} = h\left(P, P_i^{RX}, P_j^{RX}\right) - TDoA_{i,j} \\
& \Delta_M = \left[d_{2,1}^{M} \quad \cdots \quad d_{n,n-1}^{M} \right] \\
& \hat{P}_v = \arg\min_{P} \Delta_M \hat{R}_{TDoA}^{-1} \Delta_M^T
\end{aligned}
\tag{13}
$$

where $\hat{P}_v$ is the maximum likelihood estimate and $\hat{R}_{TDoA}$ is an estimate of the *TDoA* covariance given in (6). In this case the error area is given by the set of points that verify the following Chi-Square test:

$$
\Delta_M \hat{R}_{TDoA}^{-1} \Delta_M^T \le \gamma(\alpha, K) \tag{14}
$$

where $\gamma(\alpha, K)$ is the value of the Chi-Square distribution for K degrees of freedom and $1-\alpha$ confidence. Notice that for both problems in (10) and (13) we are assuming either zero *TDoA* bias, *i.e.*, $\mu_{TDoA} = 0_{Kx1}$ or that a reasonable estimate $\hat{\mu}_{TDoA}$ is available for bias compensation. This is possible in our case since the time error bias at the receiver is sufficiently stationary in time and space (Section 3). The output of the *TDoA*-based localisation procedure is a pair ($\mathbf{z}_k$, R_k). Specifically, $\mathbf{z}_k$ containing the vessel location estimate in geodetic coordinates and R_k is a covariance matrix describing the minimum volume ellipse enclosing the set of points that verify eq. (14). Time integration is then performed by using ($\mathbf{z}_k$, R_k) as inputs of a suitable Extended Kalman Filter as described in the following section.

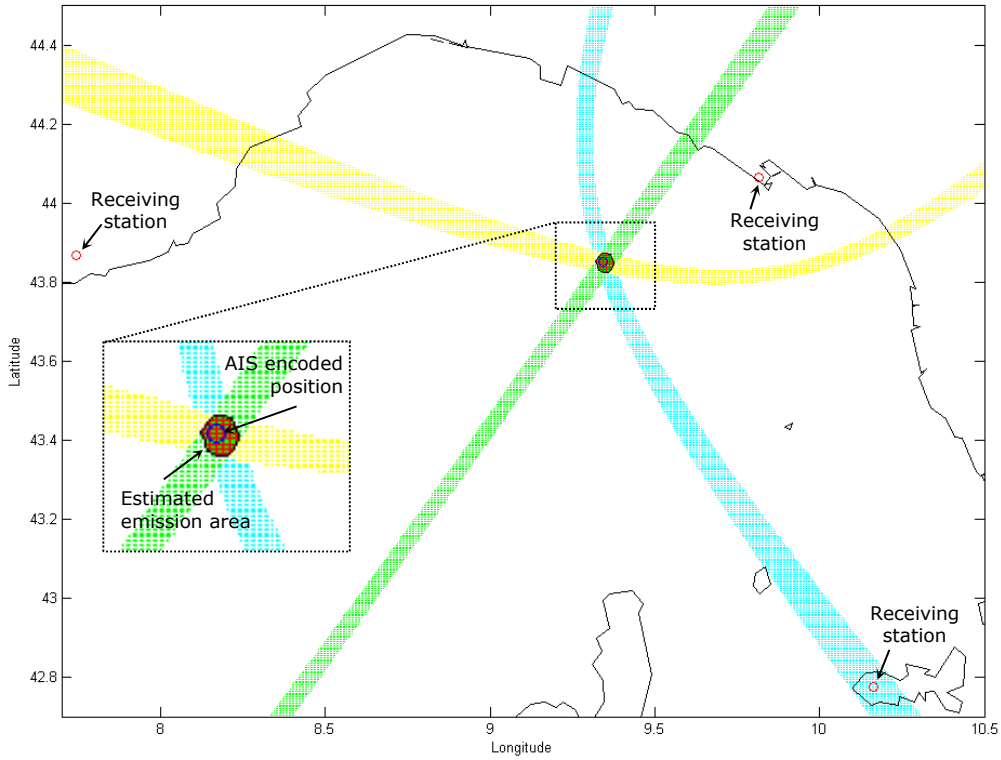

***Figure 4**: Radiolocation of the AIS emission in the Ligurian Sea as the intersection of the TDoAs hyperbolic functions between three receiving stations (red circles on land). The AIS encoded position (blue circle) falls within the estimated emission area (red).*

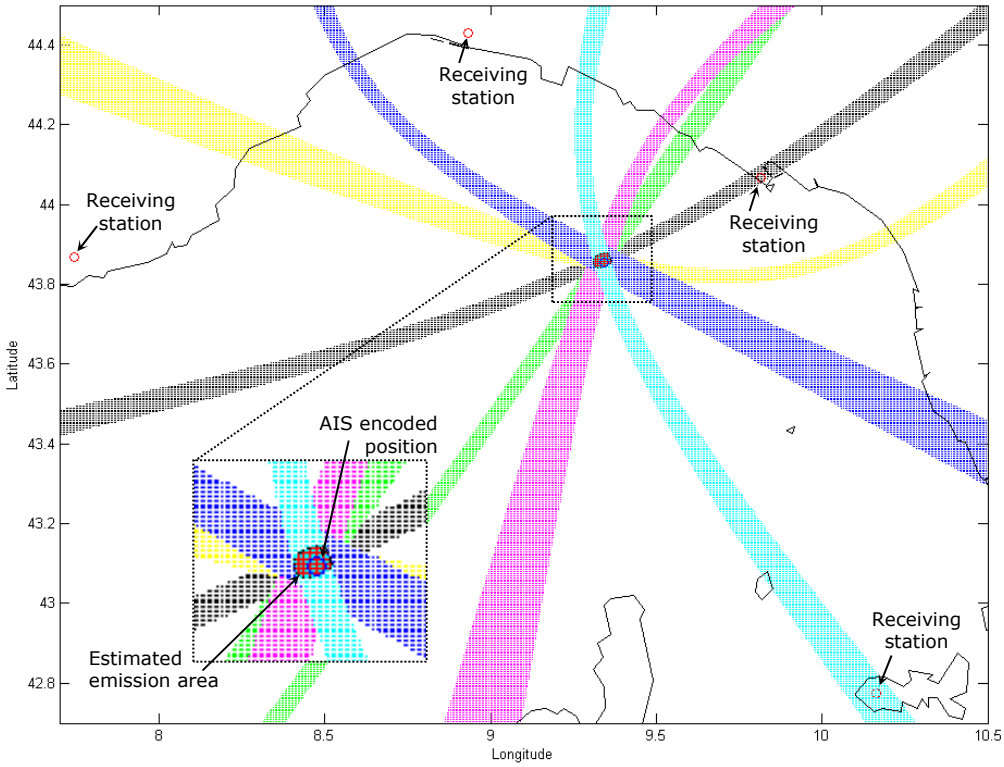

***Figure 5**: The AIS emission is received by four stations (red circles). The additional AIS base station yields a reduction of the intersection area between the available TDoAs, thus reducing the localisation uncertainty.*

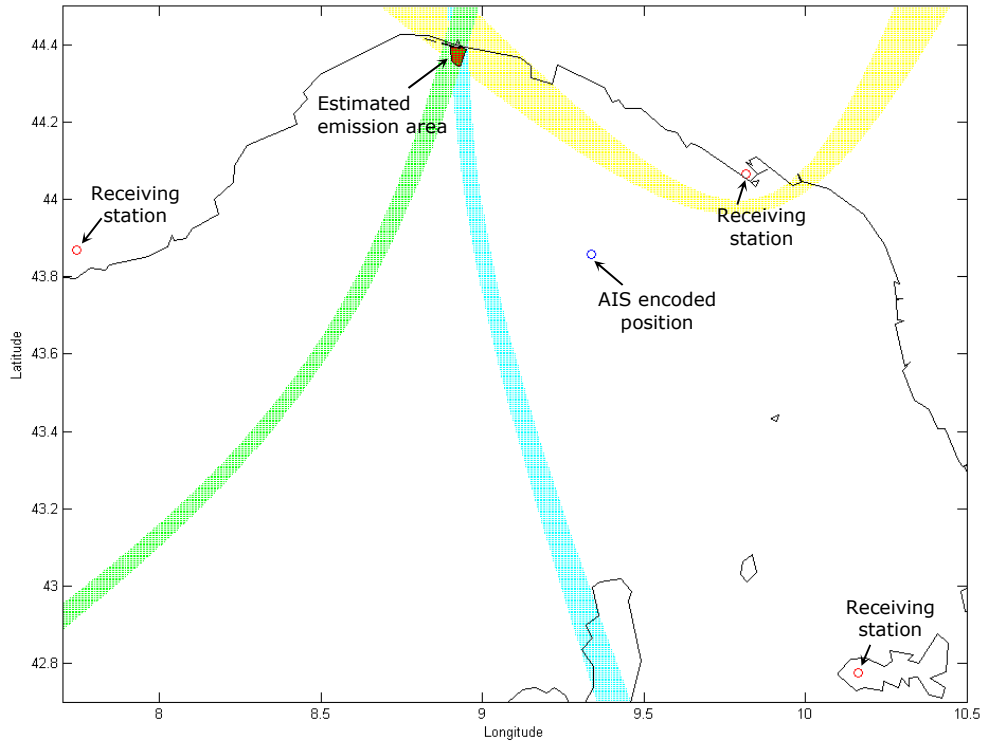

Figure 6: *The radiolocation results highlight that the message originally transmitted in open seas (blue circle) is repeated by the base station in Genoa.*

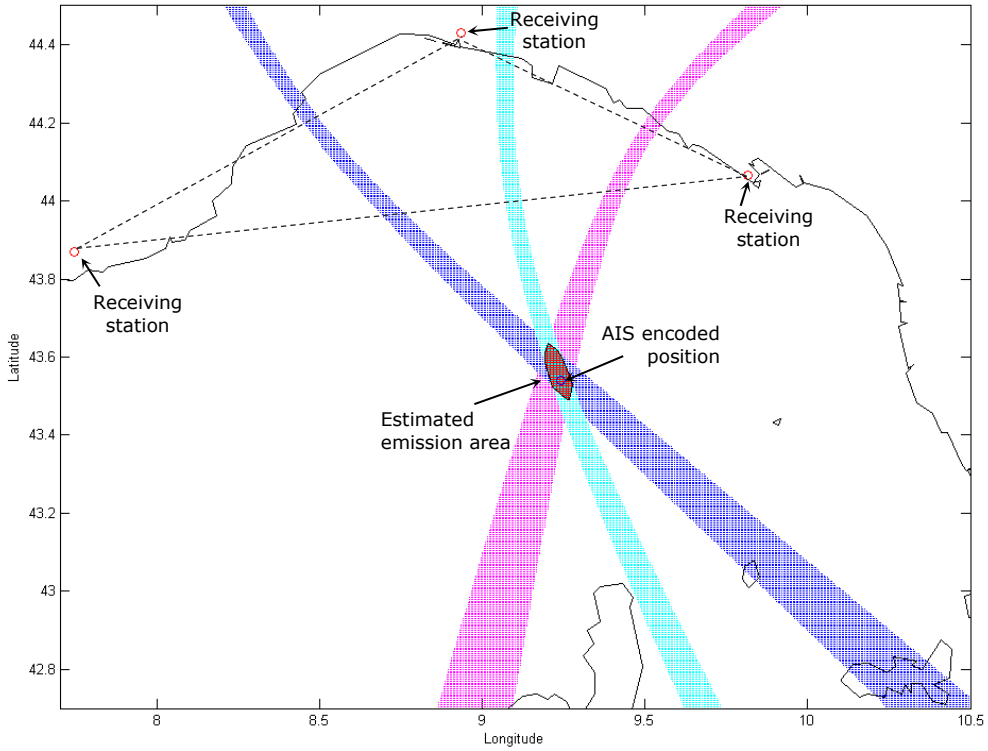

Figure 7*: The radiolocation uncertainty changes depending on the position of the emission and the receivers' location.*

Another localisation example is reported in Figure 6. Here the AIS-based radiolocation and the declared vessel position are sensibly different: this happens when the AIS message from the vessel in open seas (blue circle) is repeated by a base station[2], easily located in Genoa in this case.

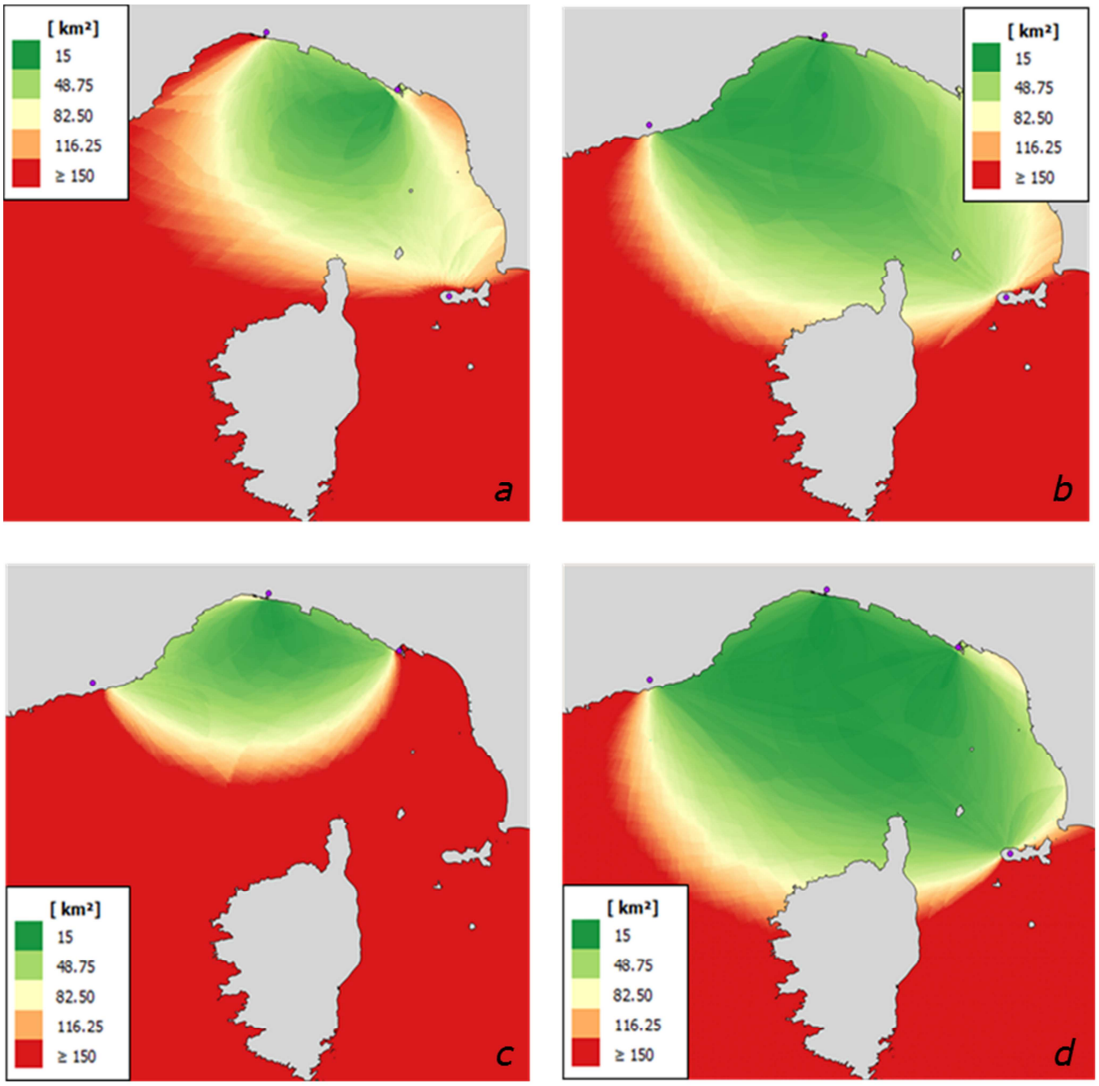

Figure 8: *Radiolocation uncertainty limits obtained when a single AIS message is received from different base stations (purple) using three TDoA measurements (a,b and c) and considering* $K = 13.5\ \mu s$ *for each TDoA. Resulting performance when the message is received by four base stations, leading to six TDoAs (d).*

The spatial distribution of base stations is central to the performance of the radiolocation process. This is given by the extent of the uncertainty at a specific location in space and varies depending on the transmitter position with respect to the receiving stations. For instance, in Figure 7 the message is received by three

[2] In accordance with AIS standard, a base station can be required to store and forward a position message sent by a vessel.

stations and the emission location can be verified. However, the error area is quite large. This happens because the vessel is far away from all the sensors baselines and the angles of arrivals are similar. To better clarify this point we performed a geometric analysis of the localisation precision with reference to the positions of the Italian Base Stations. Results are given in Figure 8, where we show how the estimated precision varies in space for different AIS network configurations.

5. Vessel Tracking using an Extended Kalman Filter

As previously mentioned, at time step k the multilateration procedure gives as output a pair $(\mathbf{z}_k, R_k)$ for each vessel, where $\mathbf{z}_k$ is the estimated vessel position and R_k its associated error covariance. We can then perform model-based time integration by recursively solving the Chapman-Kolmogorov integral and Bayes equation [22]. In fact, Bayesian methods provide a rigorous framework for dynamic state estimation problems. The idea is to construct the pdf of the system state based on all the available information, and then find an approximation of such a posteriori pdf. Classical inference methods for *nonlinear filtering* are the Extended Kalman Filter (EKF) [23], based on linearisation of the system about the current state estimate, and the Unscented Kalman Filter (UKF) [24], based on a deterministic sampling of the a posteriori pdf. Improved tracking accuracy can be generally achieved by means of Sequential Monte Carlo (SMC) methods like the Particle Filter (PF) [25].

For our specific problem we can use a nonlinear equation to efficiently describe the vessel trajectory. In fact, let x_k , y_k, v_k, and c_k be the Latitude, Longitude, Speed Over Ground (SOG), and Course Over Ground (COG) at time k. Then the geodetic vessel position at time $k+1$ is given by:

$$x_{k+1} = \frac{180}{\pi}\left(\sin\left(x_k \frac{\pi}{180} \right) \cos\left(v_k \frac{T_k}{R_{earth}} \right) + \cos\left(x_k \frac{\pi}{180} \right) \sin\left(v_k \frac{T_k}{R_{earth}} \right) \cos(c_k) \right) \tag{15}$$

$$y_{k+1} = y_k + \frac{180}{\pi} \arctan\left(\frac{\cos\left(x_k \frac{\pi}{180} \right) \sin\left(v_k \frac{T_k}{R_{earth}} \right) \sin(c_k)}{\cos\left(v_k \frac{T_k}{R_{earth}} \right) - \sin\left(x_k \frac{\pi}{180} \right) \sin\left(x_{k+1} \frac{\pi}{180} \right)} \right) \tag{16}$$

where R_{earth} is the Earth radius and T_k is the sampling interval of the filtering problem, *i.e.* the time interval between two consecutive (lat,lon) estimates from the multilateration procedure. As for the SOG v_k and COG c_k, we assume zero-dynamic with Gaussian noise. Then by choosing $\mathbf{x}_k = [x_k \; y_k \; v_k \; c_k]^T$ as the system state, we can describe our problem using the following dynamic system with nonlinear dynamics and linear measurement equation, *i.e*.

(17) $$\mathbf{x}_{k+1} = f(\mathbf{x}_k) + \mathbf{w}_k$$

(18) $$\mathbf{z}_k = H_k \mathbf{x}_k + \mathbf{v}_k$$

(18) $$H_k = \begin{bmatrix} 1 & 0 & 0 & 0 \\ 0 & 1 & 0 & 0 \end{bmatrix}$$

where $\mathbf{w}_k \sim N(0, Q_k)$ and $\mathbf{v}_k \sim N(0, R_k)$ are zero-mean white Gaussians representing the process and measurement noise, respectively. Given the initial state estimate $\mathbf{x_0}$ and associated error covariance P_0, the EKF for the system in eqs. (15)-(18) is given by the following two step recursion:

Prediction Step

(19) $$\hat{\mathbf{x}}_{k|k-1} = f(\hat{\mathbf{x}}_{k-1|k-1})$$

(20) $$P_{k|k-1} = F_{k-1} P_{k-1|k-1} F_{k-1}^T + Q_k$$

(21) $$F_{k-1} = \left. \frac{\partial f}{\partial \mathbf{x}_{k-1}} \right|_{\hat{\mathbf{x}}_{k-1|k-1}}$$

Update Step

(22) $$S_k = H_k P_{k|k-1} H_k^T + R_k$$

(23) $$K_k = P_{k|k-1} H_k^T S_k^{-1}$$

(24) $$\hat{\mathbf{x}}_{k|k} = \hat{\mathbf{x}}_{k|k-1} + K_k (\mathbf{z}_k - H_k \hat{\mathbf{x}}_{k|k-1})$$

(20) $$P_{k|k} = (I_{n \times n} - K_k H_k) P_{k|k-1}$$

where F_{k-1} in eq. (20) is the Jacobian of the nonlinear time evolution $f(\cdot)$, and $\left(\hat{\mathbf{x}}_{k|k}, P_{k|k}\right)$ are the state estimate and associated error covariance at time *k*.

Tracking Results

We now report the tracking results obtained from processing real AIS data collected by the Italian Terrestrial Network for approximately 3 hours. Results for a single vessel are depicted in Figures 9 to 11.

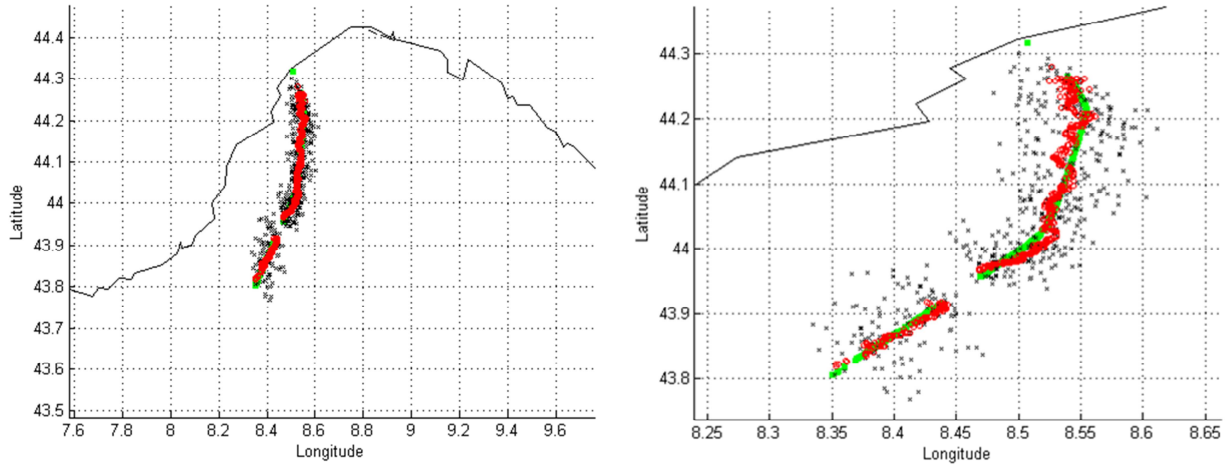

Figure 9: *Tracking results for a single vessel leaving the port of Savona (left) and zoomed trajectory. True trajectory (green), estimates from the multilateration procedure (black), and EKF position estimates (red).*

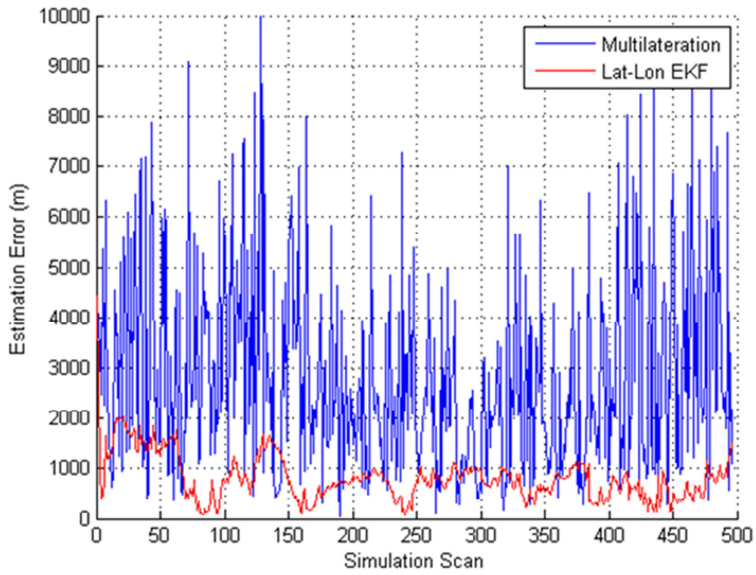

Figure 10: *Localisation error over time for a single vessel trajectory: Multilateration procedure (blue) and EKF in geodetic coordinates (red).*

Specifically, in Figure 9 we report the reference vessel trajectory (green) from GNSS data, the (lat, lon) estimates from the localisation procedure (black crosses), and the EKF position estimates (red circles). Notice that we report the reference vessel location only when the AIS message is received by at least 3 AIS base stations. This is done in order to highlight the gaps of *TDoA* measurements due to non-perfect coverage. The estimation errors over time for the *TDoA* localisation and after EKF processing are depicted in Figure 10. Finally, the EKF results in estimating the vessel kinematics, i.e. SOG and COG, are depicted in Figure 11.

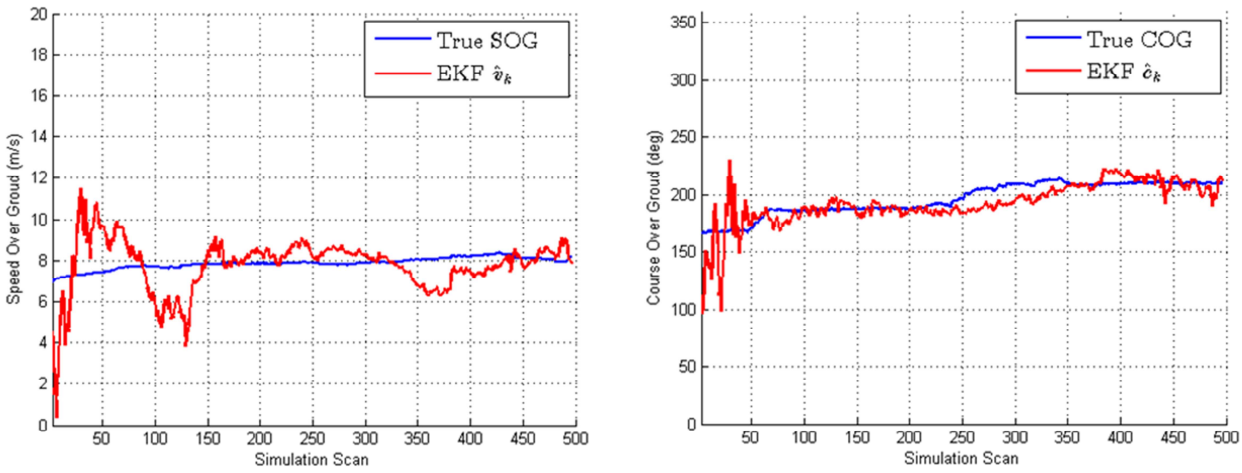

Figure 11: *EKF results in estimating the vessel kinematics. True and estimated Speed Over Ground (left); true and estimated Course Over Ground (right).*

We performed the same tracking analysis for all the vessel trajectories within the coverage of at least 3 AIS base stations. Results for a vessel leaving the port of La Spezia are depicted in Figures 12 to 14. Specifically, the (lat, lon) tracking results are depicted in Figure 12, the estimation errors are reported in Figure 13, and the EKF results in estimating the vessel COG and SOG are depicted in Figure 14. Significant differences in terms of multilateration position error can be seen from Figure 13 if compared with Figure 10 for a vessel leaving the port of Savona. This is due to better coverage in the area of La Spezia, *i.e.* there are 4 AIS base stations available most of the time, as predicted by the static analysis reported in Figure 8. The same metrics are depicted for a third vessel trajectory in Figures 15 to 17. From the results we can verify that the average

location error of the EKF is always below 2km, thus confirming the effectiveness of the radiolocation technique.

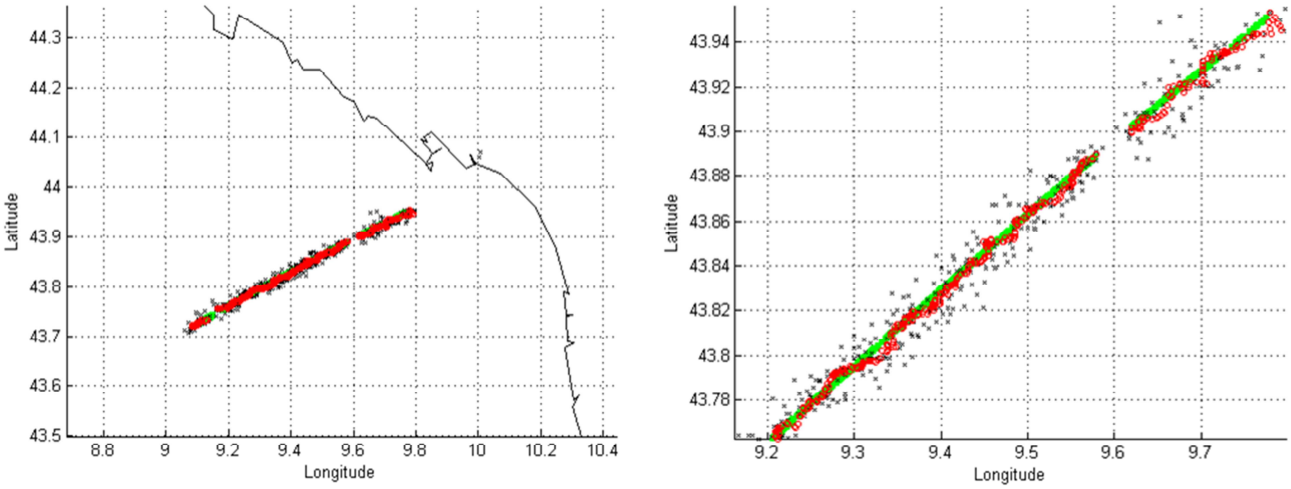

Figure 12: *Tracking results for a single vessel leaving the port of La Spezia (left) and zoomed trajectory. True trajectory (green), estimates from the multilateration procedure (black), and EKF position estimates (red).*

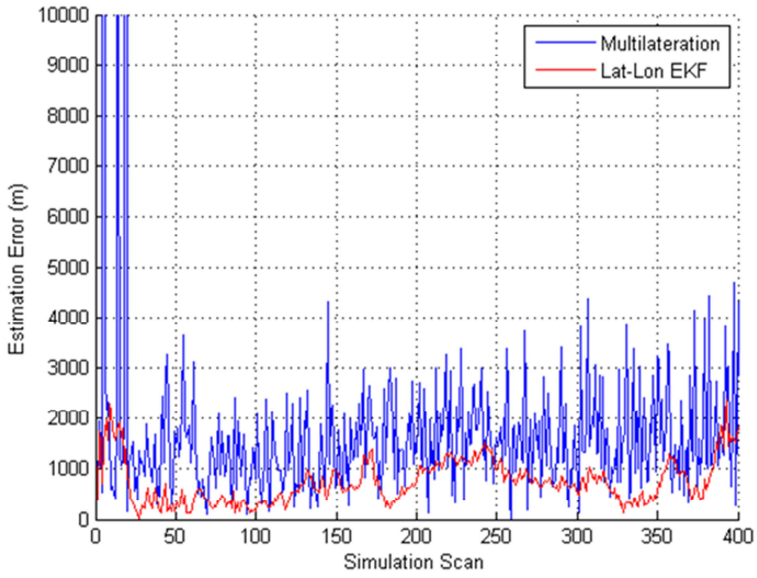

Figure 13: *Localisation error over time for a single vessel trajectory: Multilateration procedure (blue) and EKF in geodetic coordinates (red).*

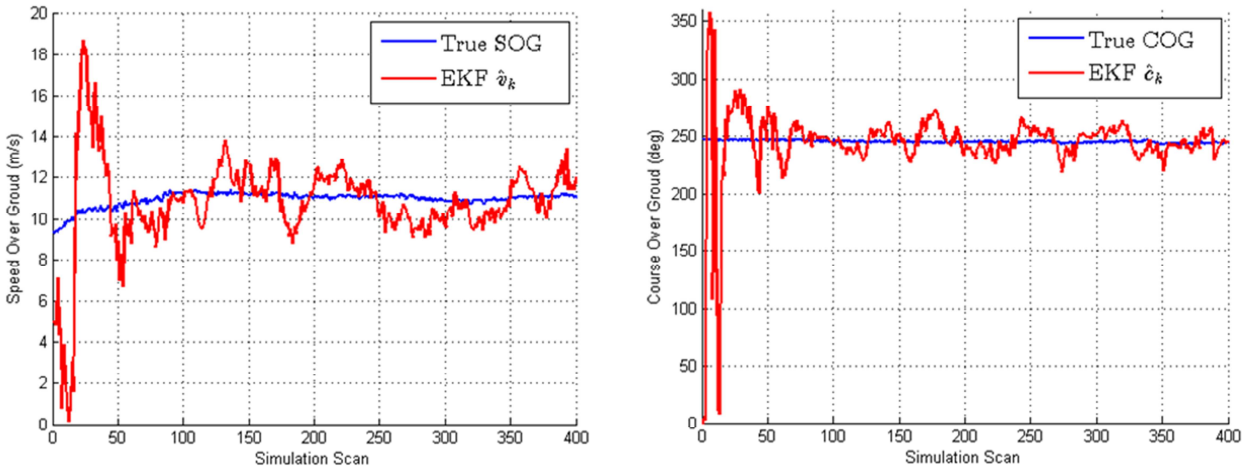

Figure 14: *EKF results in estimating the vessel kinematics. True and estimated Speed Over Ground (left); true and estimated Course Over Ground (right).*

It is worth noting that the number of scans needed by the EKF to converge to the true COG and SOG values sensibly varies from track to track. This is due to a number of factors, chief amongst them the positions of the transmitter and the receivers, the motion and velocity of the vessel and the variable time between scans. The latter depends on *i*) the AIS transmission rate, which changes according to the vessel manoeuvre and velocity and *ii*) the rate of reception of the message by three or more stations.

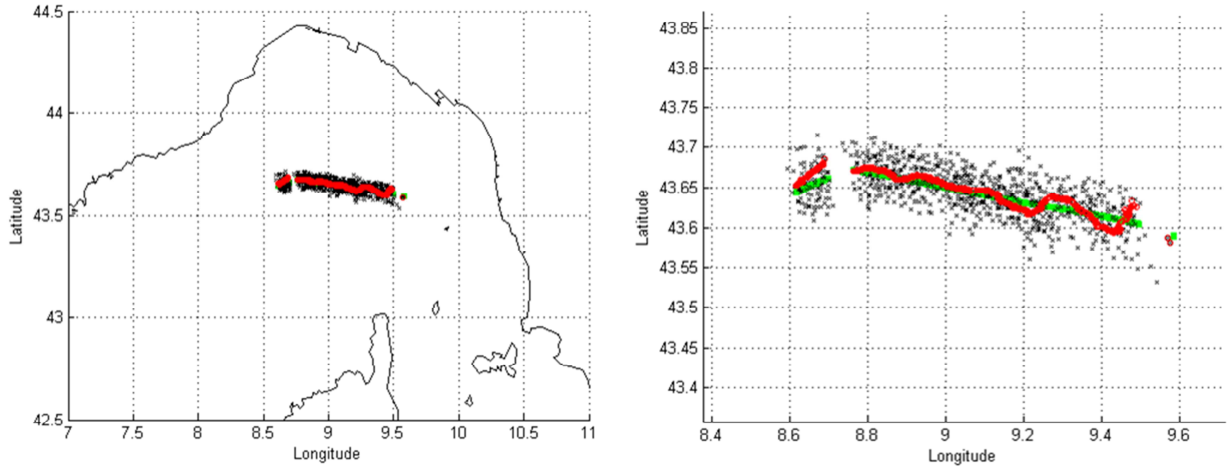

Figure 15: *Tracking results for a single vessel travelling westbound. True trajectory (green), estimates from the multilateration procedure (black), and EKF position estimates (red).*

Additional tuning of the filter parameters could lead to improved performance in terms of the estimated COG and SOG. In general reducing the filter process noise leads to more precise estimates for the vessel kinematics. This however might reduce the filter robustness and precision in terms of location estimates.

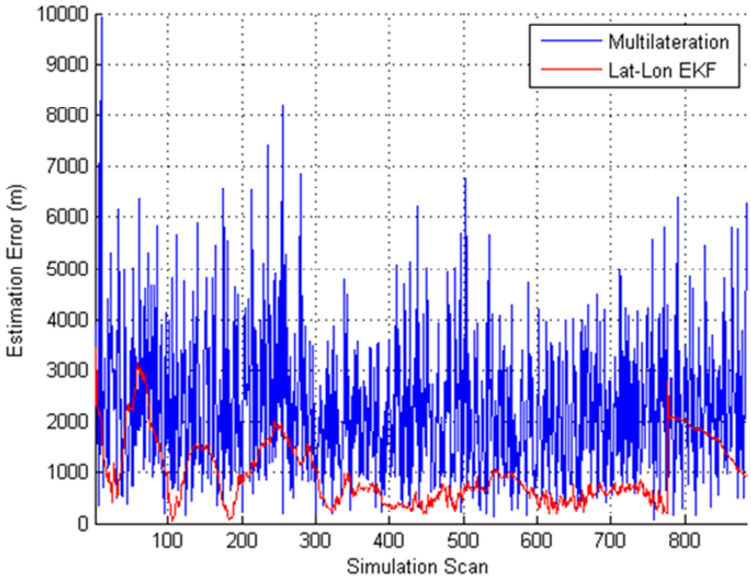

Figure 16: *Localisation error over time for a single vessel trajectory: Multilateration procedure (blue) and EKF in geodetic coordinates (red).*

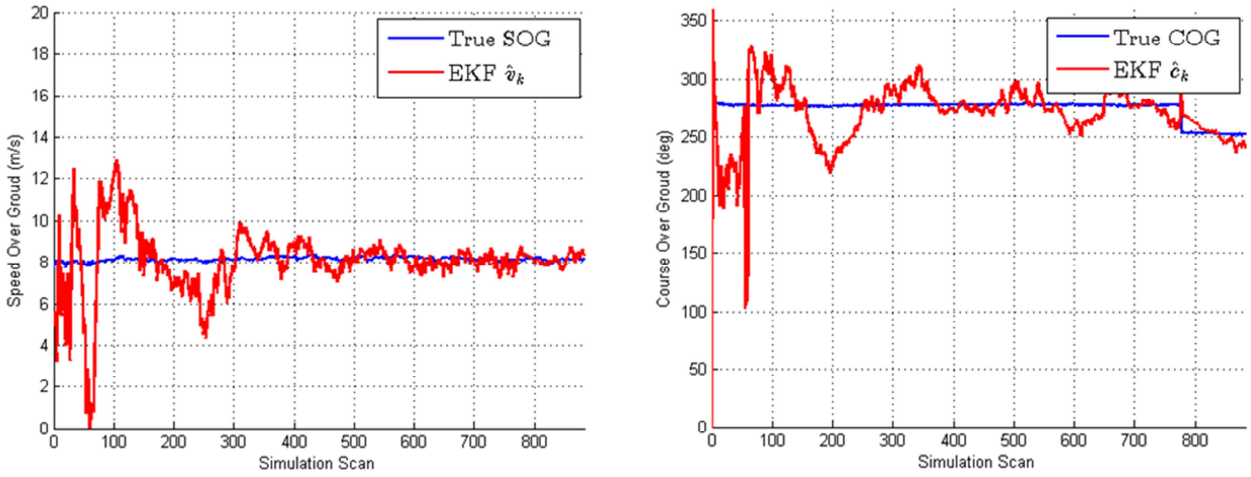

Figure 17: *EKF results in estimating the vessel kinematics. True and estimated Speed Over Ground (left); true and estimated Course Over Ground (right).*

Finally, collective results are depicted in Figure 18 where we report the tracking results for all considered vessel trajectories in the north Tyrrhenian. Specifically, we report the true vessel trajectory (green), the estimates from the multilateration procedure (black), and the EKF position estimates (red). As previously mentioned, we consider only the vessel trajectories within the coverage area of at least 3 AIS base station.

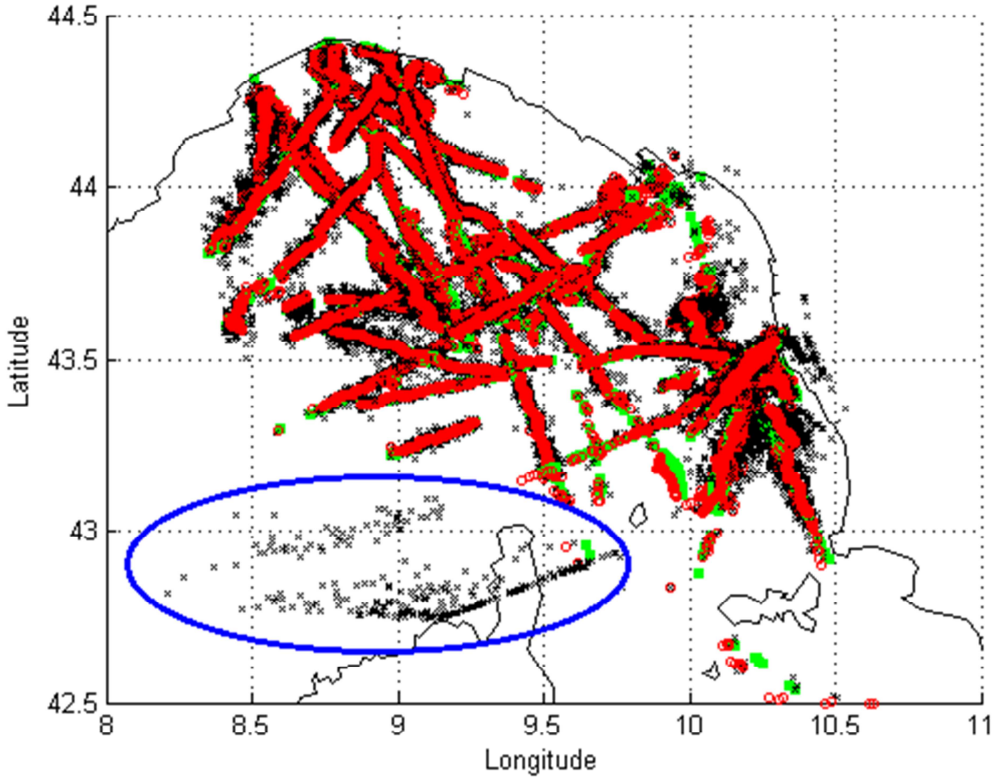

Figure 18: *Tracking results for a set of trajectories using real AIS data collected by the Italian Terrestrial Network over about 3 hours and received by 3 or more stations. It is worth noting that AIS tracks received by less than 3 stations are not plotted.*

Two final remarks on the results in Figure 18: (1) some of the estimates from the multilateration procedure are on land; this is due to the fact that the multilateration procedure is performed without applying land constraints to avoid biasing the EKF measurements. However, Bayes optimal methods to enforce such constraints exist [26] and will be used in future developments. (2) Some of the initial/final estimates from the multilateration procedure are far away from the true vessel location (blue highlight in the figure): this happens when there is a non-optimal spatial distribution of the AIS base stations, leading to multiple solutions (*ghost estimates*) to the *TDoA* localisation problem. This problem could be solved by extending the overlapping coverage of the AIS network and/or by using a Sequential Monte Carlo (SMC) filter, e.g. the

Particle Filter, to keep track of the intrinsically multimodal posterior pdf. We will in fact consider the use of Particle Filtering for future research since it should lead to more robust results for decision making.

The demonstrated average performance of the proposed radiolocation and tracking technique based on EKF confirms that the approach could be used to perform automatic validation of declared GNSS positions encoded in the broadcast AIS messages. This could be performed using a single step gate validation [27] or a more effective binary hypothesis testing over a moving time window [28]. The former approach may be sufficient if the EKF estimate is close to the true vessel position but is intrinsically prone to a large number of false positives. A more effective way of performing data validation is the use of a binary hypothesis test where H_1 is the hypothesis for no anomaly and H_0 the hypothesis for ongoing anomaly. Given the random variable Z representing the multilateration output and z its realization, the binary hypothesis test is performed by comparing the likelihood ratio $p_{z|H_1}(Z|H_1)/p_{z|H_0}(Z|H_0)$ against a decision threshold defined by the prior and Bayes risk [28]. In particular, the $p_{z|H_1}(Z|H_1)$ represents the likelihood of observing z given the vessel is located in the GNSS declared position, and $p_{z|H_0}(Z|H_0)$ is the likelihood of observing z given the vessel is following the EKF estimated track. Both the single step validation gate and the binary hypothesis test should be applied only when the multilateration confidence is high (see Figure 8) in order to minimise the anomaly false alarm rate. These aspects will be the subject of future research activities.

6. Conclusions

A number of activities (traffic monitoring & management, Search & Rescue, etc.) at sea are based upon information provided by vessels through AIS. AIS communication system is prone to tampering and spoofing, thus the validation of the data provided through a reporting system such as AIS is an important issue faced by authorities involved in the different areas of maritime surveillance. It is not known the level of actual alteration of AIS provided data which, nevertheless, is expected to increase in the future. Therefore, it is important to improve the assessment of the reliability of the position data transmitted by ships in an automated way to increase the safety of the seas. This paper has successfully addressed this issue offering an effective method to validate the position data sent by the ships through AIS, with an accuracy that ranges from few hundreds of metres, in optimal condition, to few kilometres in marginal situation. It has to be noted that from the operational point of view such accuracy can be considered more than acceptable. The proposed

method collects the data provided by the network of stations receiving the AIS messages transmitted by the ship at seas and uses the Time Stamp (Time of Arrival) added by the AIS base stations to the messages received from the ship. The algorithm allows, in few steps, to narrow down the estimated position of the ship to few hundreds of metres (without using in any way the position reported by the ship). The algorithm described in the paper has been successfully tested using real, anonymised data provided by the Italian Coast Guard, demonstrating that EKF outperforms multilateration for maritime situational awareness. Moreover, the tracks originated by the proposed methodology can be thought of as the input of automatic tools for the detection of anomalies related to AIS data verification, which represent the next stage of this research activity.

Acknowledgements

The authors would like to thank the reviewers for their valuable contribution in improving the paper.

References

[1] Angrisano, A., Gaglione, S., Gioia, C.: 'Performance assessment of aided Global Navigation Satellite System for land navigation', IET Radar, Sonar & Navigation, 2013, 7(6), pp. 671-680

[2] Safety of Life at Sea (SOLAS) convention Chapter V, Regulation 19.

[3] Directive 2002/59/EC of the European Parliament and of the Council establishing a Community vessel traffic monitoring and information system, as amended by Directive 2009/17/EC and Commission Directive 2011/15/EU.

[4] Baldauf, M., Benedict, K., Motz, F.: 'Aspects of technical reliability of navigation systems and human element in case of collision avoidance', Proc. Navigation Conference & Exhibition, 2008

[5] Høye, G. K., Eriksen, T., Meland, B. J., Narheim, B. T.: 'Space-based AIS for global maritime traffic monitoring' Acta Astronautica, 62(2), 2008, pp. 240-245

[6] Pallotta, G., Vespe, M., Bryan, K.: 'Vessel Pattern Knowledge Discovery from AIS Data: A Framework for Anomaly Detection and Route Prediction', Entropy, 15(6), 2013, pp. 2218-2245

[7] Ristic, B., La Scala, B., Morelande, M., Gordon, N.: 'Statistical analysis of motion patterns in AIS data: Anomaly detection and motion prediction', Proc. 11th IEEE Int. Conf. on Information Fusion, 2008

[8] Roy, J.: 'Anomaly detection in the maritime domain', SPIE Defense and Security Symposium, International Society for Optics and Photonics, 2008

[9] Kroener, U., Dimc, F.: 'Hardening of civilian GNSS trackers', Proc of the 3rd GNSS Vulnerabilities and Solutions Conference, 2010.

[10] ‘Ship Tracking Hack Makes Tankers Vanish from View’, ww.technologyreview.com/news/520421/ship-tracking-hack-makes-tankers-vanish-from-view, accessed July 2006

[11] Guerriero, M., Willett, P., Coraluppi, S., Carthel, C.: ‘Radar/AIS data fusion and SAR tasking for maritime surveillance’, Proc. 11th IEEE Int. Conf. on Information Fusion, 2008

[12] Katsilieris, F., Braca, P., & Coraluppi, S.: ‘Detection of malicious AIS position spoofing by exploiting radar information’, Proc. 16th IEEE Int. Conf. on Information Fusion, 2013, pp. 1196-1203

[13] Vespe, M., Sciotti, M., Burro, F., Battistello, G., Sorge, S.: ‘Maritime multi-sensor data association based on geographic and navigational knowledge’, Proc. IEEE Radar Conference, 2008

[14] TRITON (TRusted vessel Information from Trusted On-board iNstrumentation) project, funded by the EU within the Seventh Framework Programme (FP7)

[15] Chan, Y. T., Ho, K. C.: ‘A simple and efficient estimator for hyperbolic location’, IEEE Transactions on Signal Processing, , 42(8), 1994, 1905-1915

[16] Gustafsson, F., Gunnarsson, F.: ‘Positioning using time-difference of arrival measurements’, Proc. IEEE Int. Conf. on Acoustics, Speech, and Signal Processing, 2003, Vol. 6, pp. VI-553

[17] Pourvoyeur, K., Mathias, A., Heidger, R.: ‘Investigation of measurement characteristics of MLAT/WAM and ADS-B’, Proc. IEEE Tyrrhenian Int. Workshop on Digital Communications-Enhanced Surveillance of Aircraft and Vehicles, 2011, pp. 203-206

[18] Galati, G., Gasbarra, M., Magaro, P., De Marco, P., Mene, L., Pici, M.: ‘New Approaches to Multilateration processing: analysis and field evaluation’. Proc. 3rd IEEE European Radar Conference, 2006, pp. 116-119

[19] Recommendation ITU-R M 1371-4, ‘Technical characteristics for a universal shipborne automatic identification system using time division multiple access in the VHF maritime mobile band’

[20] IEC 62320-1, Maritime navigation and radiocommunication equipment and systems – Automatic Identification System (AIS) – Part 1: AIS Base Stations – Minimum operational and performance requirements, methods of testing and required test results

[21] Kay, S.M.: ‘Fundamentals of Statistical Signal Processing: Estimation Theory’. Prentice Hall Inc., 1993

[22] Anderson, B. D., Moore, J. B.: ‘Optimal filtering’ Courier Dover Publications, 2012

[23] Bar-Shalom, Y., Fortmann, T.: ‘Tracking and Data Association’, Mathematics in Science and Engineering’, vol. 179. Academic Press, 1988

[24] Julier, S. J., Uhlmann, J. K.: ‘Unscented filtering and nonlinear estimation’, Proceedings of the IEEE, 92(3), 2004, pp. 401-422

[25] Gordon, N. J., Salmond, D. J., & Smith, A. F. (1993, April). Novel approach to nonlinear/non-Gaussian Bayesian state estimation. In IEE Proceedings F (Radar and Signal Processing) (Vol. 140, No. 2, pp. 107-113). IET Digital Library.

[26] Papi, F., Podt, M., Boers, Y., Battistello, G., Ulmke, M.: 'On constraints exploitation for particle filtering based target tracking'. In Information Fusion (FUSION), Proc. 15th IEEE Int. Conf. on Information Fusion, 2012, pp. 455-462

[27] Bar-Shalom, Y., Willett, P. K., Tian, X., "Tracking and Data Fusion: A Handbook of Algorithms", YBS Publishing, 2011

[28] Van Trees H. L.: 'Detection, Estimation, and Modulation Theory: Radar-Sonar Signal Processing and Gaussian Signals in Noise', Krieger Publishing Co., 1992